Supplement of

Wall loss of semi-volatile organic compounds in a Teflon bag chamber for the temperature range of 262-298 K

Longkun He[1], Wenli Liu[2], Yatai Li[1,3], Jixuan Wang[1], Mikinori Kuwata[2], Yingjun Liu[1]

[1]State Key Joint Laboratory of Environmental Simulation and Pollution Control, College of Environmental Sciences and Engineering, Peking University, Beijing, 100871, China
[2]Department of Atmospheric and Oceanic Sciences and Laboratory for Climate and Ocean-Atmosphere Studies, School of Physics, Peking University, Beijing 100871, China
[3]Now at College of Public Health, Zhengzhou University, Zhengzhou, 450001, China

Correspondence to: Mikinori Kuwata (kuwata@pku.edu.cn), Yingjun Liu (yingjun.liu@pku.edu.cn)

Table S1. List of n-alkanes used for the present study, along with the saturation vapor pressure at 298 K predicted by the EVAPORATION group contribution method (Compernolle et al., 2011). All the chemicals were purchased from Konoscience.

compound name	carbon number	CAS number	purity	saturation vapor pressure (Pa)
n-tetradecane	14	629-59-4	99%	2.8E+00
n-pentadecane	15	629-62-9	98%	9.2E-01
n-hexadecane	16	544-76-3	98%	3.0E-01
n-heptadecane	17	629-78-7	99%	1.0E-01
n-octadecane	18	593-45-3	99%	3.3E-02
n-nonadecane	19	629-92-5	98%	1.1E-02

Table S2. Abundances of diisobutyl phthalate (DiBP) and dibutyl phthalate (DnBP) in the chamber and outside of the chamber (*i.e.*, room air in the laboratory) detected by the SV-TAG during one experiment at room temperature. The chemical species were selected, as they were abundant in the room air of the laboratory. The minimum concentration in the chamber bag suggests that intrusion of the room air into the experimental setup was minimal. Peak areas were integrated by Agilent MassHunter Station Quantitative Analysis (10.0, Agilent Technologies, Inc.).

time after injection (min)	peak area (counts)		ratio of inside chamber to room air	
	DiBP	DnBP	DiBP	DnBP
chamber background (0)	15618	12532	0.44%	0.47%
73	16197	15266	0.46%	0.57%
133	19457	24483	0.55%	0.91%
206	18029	20958	0.51%	0.78%
406	18920	21996	0.53%	0.82%
553	13110	13526	0.37%	0.50%
733	13073	11923	0.37%	0.45%
936	14189	12866	0.40%	0.48%
Reference value for the room air	3539783	2679338	-	-

Table S3. Optimized parameter sets of the two-layer model used in Figure 3. Best-fit parameter sets were obtained by the Newton method via Wolfram Mathematica 13.1.

Compound	forward rate, k_1 (min^{-1})	backward rate, k_{-1} (min^{-1})	first-order loss rate, k_2 (min^{-1})[a]
C$_{14}$ n-alkane	0.017	0.012	0.0006
C$_{15}$ n-alkane	0.017	0.012	0.0011
C$_{16}$ n-alkane	0.020	0.011	0.0016
C$_{17}$ n-alkane	0.028	0.011	0.0022
C$_{18}$ n-alkane	0.038	0.013	0.0026
C$_{19}$ n-alkane	0.070	0.013	0.0028

a. k_2 obtained here was not used in Section 3.3 (characterization of diffusion in the Teflon wall). These fitting overestimated the first-order loss rate constant for low volatile species, C$_{16}$ – C$_{19}$ n-alkanes, as shown in Figure 3.

Table S4. List of investigated chemical species by each study in Figure 6.

Source	chemical species
This work	*n*-alkanes
Yeh and Ziemann (2015)	2-ketones, 2-alcohols, monoacids, and 1,2-diols
Matsunaga and Ziemann (2010)	*n*-alkanes and 1-alkenes
Yeh and Ziemann (2014)	alkylnitrates
Krechmer et al. (2016)	dihydroxynitrates (DHNs), dihydroxycarbonylnitrates (DHCNs), and tri-hydroxynitrates (THNs)
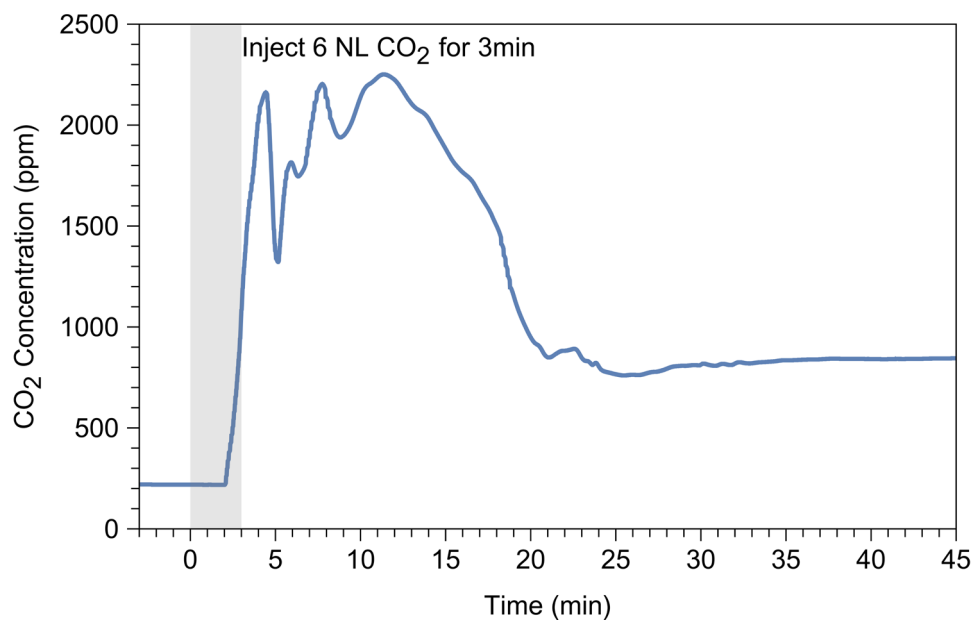
Figure S1. Time series of CO_2 concentration in the Teflon chamber for the experiment of testing the chamber volume. 6 NL (normal condition volume, at 273.15 K) of CO_2 was injected during the first 3 mins (gray area in the figure). CO_2 concentration was continuously measured by a CO_2 analyzer (SBA-5, PP System Inc.) at the opposite side of the chamber. The bag volume was determined to be 990 L at room temperature by the change in the CO_2 concentration. The measured volume was used in data analysis. The time scale for the complete mixing of CO_2 was approximately 30 mins.
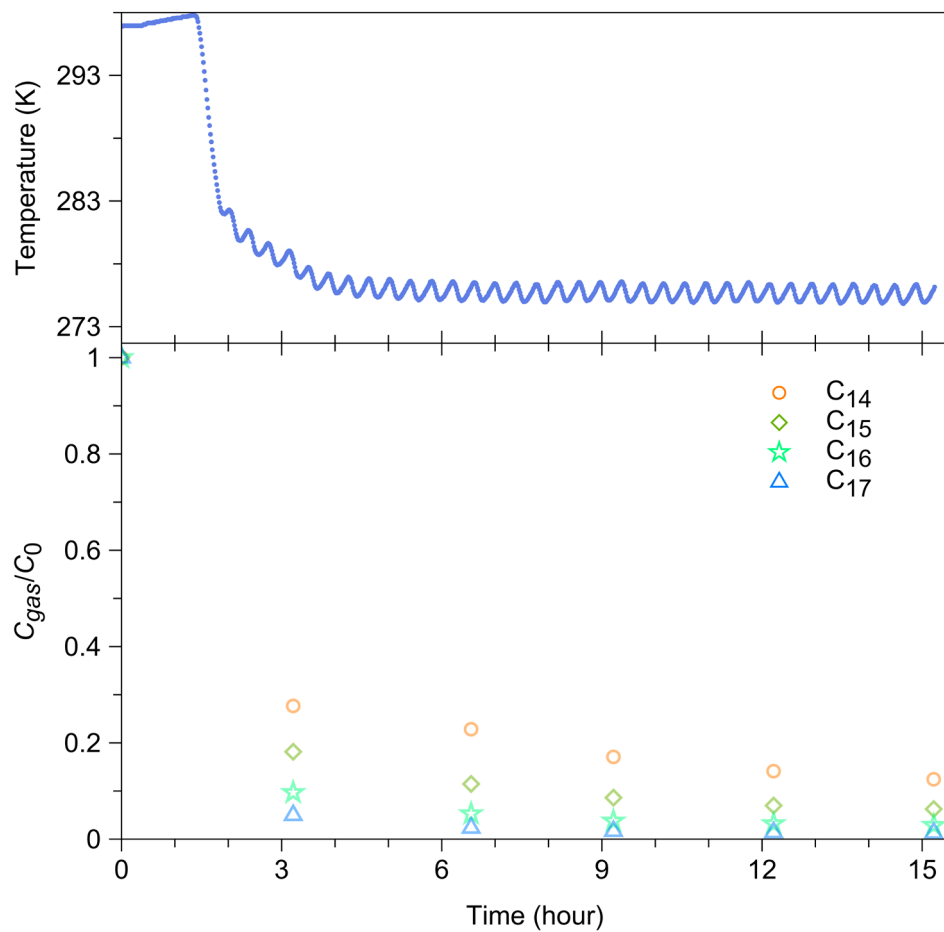
Figure S2. The values of C_{gas}/C_0 for C_{14}-C_{17} *n*-alkanes measured in the gas phase for the experiment at 275.7 ± 0.5 K. The freezer was turned on after 1 hour of the completion of the injection.
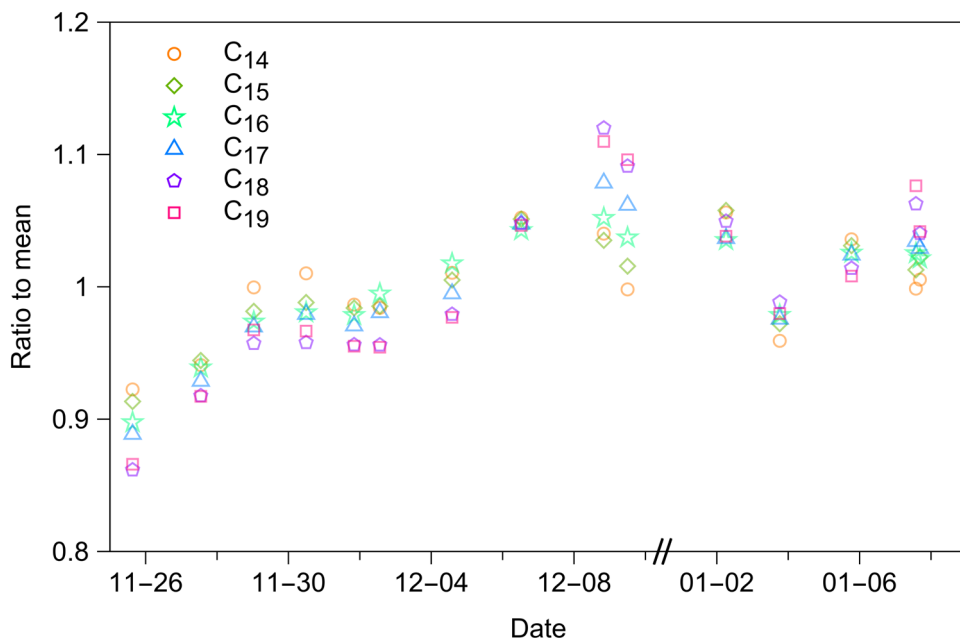
Figure S3. Relative changes in the peak areas of the standard *n*-alkanes solution during the experiment period. The data suggested that the sensitivity of the SV-TAG was stable within the fluctuation of ± 10%.
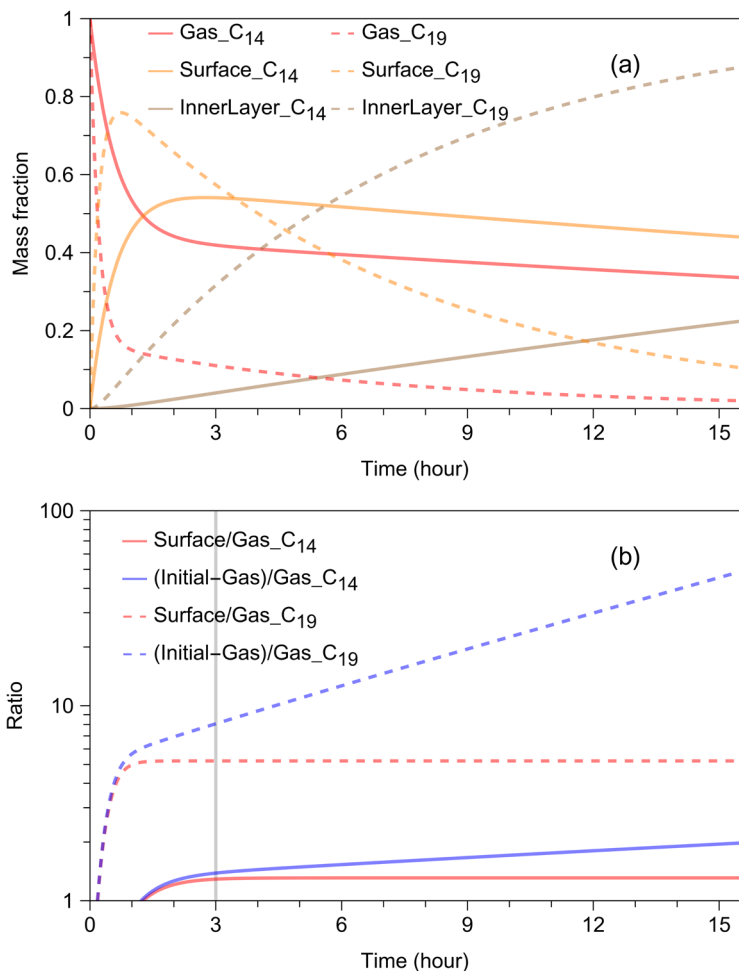
Figure S4. Simulation results of the two-layer model for room temperature experiment (Figure 3). (a) Time series of mass fraction of the total injection in gas, surface, and inner layer phases for C_{14} and C_{19} *n*-alkanes. Solid and dashed lines represent C_{14} and C_{19} *n*-alkanes respectively. Red, orange, and brown lines represent mass fractions in gas, surface, and inner layer phases respectively. (b) Time series of the ratio of mass in surface and gas phase and the ratio of mass not in and in the gas phase for C_{14} and C_{19} *n*-alkanes. Solid and dashed lines represent C_{14} and C_{19} *n*-alkanes respectively. Red and blue lines represent the theoretical and measured $C_{surface}/C_{gas}$ in the main text respectively. The gray solid line indicates 3 hours as we choose the 3-hour measurements to calculate $C_{surface}/C_{gas}$ in the main text.
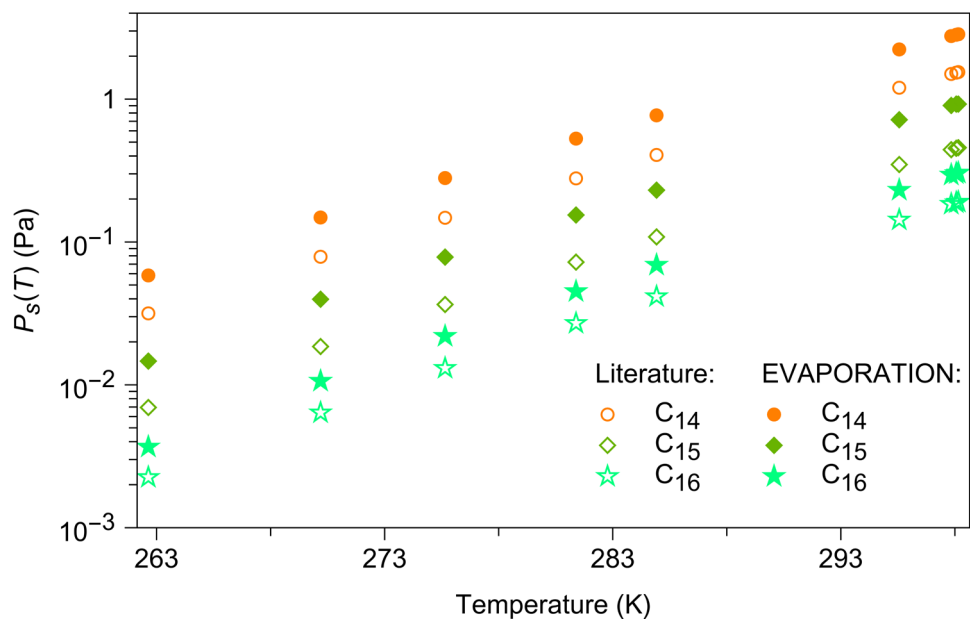
Figure S5. Saturation vapor pressures at different experimental temperatures for C_{14}-C_{16} *n*-alkanes calculated by the EVAPORATION method (Compernolle et al., 2011) and the Clausius–Clapeyron equation with literature values (Fitzpatrick, 2004; Rumble, 2022).

Text S1. Uncertainty in $C_{surface}/C_{gas}$ by employment of 3-hour measurement data.

Uncertainties in $C_{surface}/C_{gas}$ for C_{14} and C_{19} n-alkanes at room temperature by employment of the 3-hour measurement data are shown in Figure S4b. The discrepancy between the red lines and corresponding blue lines at 3 hours is the bias caused by the employment of 3-hour measurements. For C_{14} and C_{19} n-alkanes, this method overestimates 7% and 55 %. A more extreme case was used to simulate the low-temperature experiment by employing 10 times at k_1 of C_{19} n-alkane and the maximum k_2 in all the experiments. In this case, this method overestimates $C_{surface}/C_{gas}$ within 62 % of the theoretical values.

Reference

Compernolle, S., Ceulemans, K., and Muller, J. F.: EVAPORATION: a new vapour pressure estimation methodfor organic molecules including non-additivity and intramolecular interactions, Atmos. Chem. Phys., 11, 9431-9450, https://doi.org/10.5194/acp-11-9431-2011, 2011.

Fitzpatrick, R. B.: Haz-Map, Medical Reference Services Quarterly, 23, 49-56, https://doi.org/10.1300/J115v23n02_05, 2004.

Krechmer, J. E., Pagonis, D., Ziemann, P. J., and Jimenez, J. L.: Quantification of Gas-Wall Partitioning in Teflon Environmental Chambers Using Rapid Bursts of Low-Volatility Oxidized Species Generated in Situ, Environ. Sci. Technol., 50, 5757-5765, https://doi.org/10.1021/acs.est.6b00606, 2016.

Matsunaga, A. and Ziemann, P. J.: Gas-Wall Partitioning of Organic Compounds in a Teflon Film Chamber and Potential Effects on Reaction Product and Aerosol Yield Measurements, Aerosol Sci. Technol., 44, 881-892, https://doi.org/10.1080/02786826.2010.501044, 2010.

Rumble, J.: CRC handbook of chemistry and physics, CRC press, ISBN978-1032121710, 2022.

Yeh, G. K. and Ziemann, P. J.: Alkyl Nitrate Formation from the Reactions of C-8-C-14 n-Alkanes with OH Radicals in the Presence of NOx: Measured Yields with Essential Corrections for Gas-Wall Partitioning, J. Phys. Chem. A, 118, 8147-8157, https://doi.org/10.1021/jp500631v, 2014.

Yeh, G. K. and Ziemann, P. J.: Gas-Wall Partitioning of Oxygenated Organic Compounds: Measurements, Structure-Activity Relationships, and Correlation with Gas Chromatographic Retention Factor, Aerosol Sci. Technol., 49, 726-737, https://doi.org/10.1080/02786826.2015.1068427, 2015.